

# Electrochemical and XAFS Studies of Effects of Carbonate on the Oxidation of Arsenite

JAESHIN KIM,<sup>†</sup> GREGORY V. KORSHIN,<sup>\*,†</sup>  
ANATOLY I. FRENKEL,<sup>‡</sup> AND  
ALEXANDER B. VELICHENKO<sup>§</sup>

*Department of Civil and Environmental Engineering  
Box 352700, University of Washington,  
Seattle, Washington 98115-2700, Physics Department,  
Yeshiva University, 245 Lexington Avenue,  
New York, New York 10016, and Department of Physical  
Chemistry, Ukrainian State University of Chemical  
Technology, Gagarin Ave., 8 Dnepropetrovsk 49005 Ukraine*

Measurements of electrochemical (EC) arsenite oxidation demonstrated that the arsenite oxidation current increased in the presence of carbonate while the potential of the onset of EC arsenite oxidation exhibited a strong shift toward less positive values. Examination of pH and total carbonate concentration effects on the EC arsenite oxidation parameters showed that they were affected solely by the concentration of carbonate ion  $\text{CO}_3^{2-}$ , which appeared to form relatively weak mono- and dicarbonate complexes with arsenite. The EC activity of these complexes was determined to be almost an order of magnitude higher than that of free arsenite. However, X-ray absorption fine-structure (XAFS) measurements did not show any changes in the properties of the As(III) inner complexation shell associated with the presence of the bound carbonate ions. It was accordingly concluded that the strength of bonds between the bound carbonate and As(III) is close to that for As(III)–OH<sup>−</sup> interactions. The acceleration of the oxidation of carbonate–As(III) complexes was hypothesized to be associated with an additional pathway of the formation of As(IV) intermediates, in which the carbonate group present in the As(III) inner shell provides an electron to form a bound carbonate radical and also a good leaving group for facile cleavage from the transient As(IV) species.

## Introduction

Arsenic in drinking water has been associated with a variety of adverse effects. In some cases, notably in Bangladesh, West Bengal, and possibly Vietnam, exposures to arsenic have resulted in a full-scale epidemic of arsenicosis (1, 2). Treatment methods developed to remove water-borne arsenic and to prevent or alleviate health crises associated with it (3–6) tend to perform very well for arsenate while the removal of the predominant inorganic form of reduced arsenic, arsenite, associated *inter alia* with higher toxicity and carcinogenicity is more difficult. The removal of arsenic can be improved via arsenite oxidation that can be carried out using homogeneous or heterogeneous processes (using

MnO<sub>2</sub>-based media or electrochemical, EC, systems) (7–14). The kinetics of arsenite oxidation in these processes is strongly affected by pH, concentrations of arsenite, iron, dissolved oxygen, H<sub>2</sub>O<sub>2</sub>, and carbonate (9–11).

The role of carbonate in arsenite oxidations and in the environmental chemistry of arsenic at large has not been specifically explored but it appears to be notable. For instance, arsenic release into groundwater increases for carbonate concentrations above ca. 200 mg/L (15–17), most likely because of the competition between arsenate and carbonate for surface adsorption sites. On the other hand, increase of arsenic release at elevated carbonate concentrations has been hypothesized to be a result of the formation of carbonate complexes of As(III) with assumed stoichiometries  $\text{AsCO}_3^+$ ,  $\text{As}(\text{CO}_3)_2^-$ , and  $\text{As}(\text{CO}_3)(\text{OH})_2^-$  (18). The issue of whether the formation of these complexes affects the kinetics of arsenite oxidation has not been addressed, but it has been determined that the oxidation of arsenite by, for instance, molecular oxygen, hydrogen peroxide, or in EC reactors is promoted at increased carbonate concentrations (9–11, 14). Detailed kinetic models of arsenite oxidations (9–11, 19) do not include carbonate complexes of As(III) into the reaction sequences, but they presume that the oxidation of arsenite proceeds through the formation of unstable As(IV) intermediates.

The assumption that the oxidation of arsenite involves the formation of As(IV) species is based on the results of pulse radiolysis, photochemical, and EC experiments (19–24). The As(IV) species were reported to be predominated by  $\text{As}(\text{OH})_4$  and  $\text{H}_2\text{AsO}_3$  that coexist in a dynamic pH-dependent equilibrium and their deprotonated forms (primarily  $\text{As}(\text{OH})_3\text{O}^-$  and  $\text{HASO}_3^-$  at pH > 8). As(IV) species either undergo disproportionation in rapid second-order reaction to form As(III) and As(V) or they can be oxidized by molecular oxygen and other available oxidants.

EC voltammetric experiments have also shown that the oxidation of arsenite involves two one-electron charge-transfer reactions that manifest themselves as distinct features in the potentiodynamic scans (22–24). Formation of an As(IV) intermediate was also assumed to take place in EC oxidations. However, neither currently available EC nor pulse radiolysis data are detailed enough to quantify the effects of carbonate in the oxidation of arsenite. The goal of this study was to carry out consistent examination of the effects of carbonate in the oxidation of arsenite and formation of arsenic intermediates.

## Materials and Methods

Methods employed in this study included EC voltammetry at platinum and gold rotating disk electrodes (RDE) and X-ray absorption fine-structure spectroscopy (XAFS). EC measurements were performed using a Pine AFMSRX rotator and a Pine AFCBP1 bipotentiostat (Pine Instrument Co., Grove City, PA) or a Cypress CS-1200 (Cypress Systems, Inc., Lawrence, KS) potentiostat. A conventional three-compartment EC cell was employed. The temperature was  $25 \pm 1^\circ\text{C}$ . All potentials are quoted versus the saturated calomel electrode (SCE). The surface areas of the Pt and Au electrodes were 0.50 and 0.16 cm<sup>2</sup>, respectively. Before each measurement, the electrodes were treated for 2 min in a 1:1 mixture of concentrated H<sub>2</sub>SO<sub>4</sub> and H<sub>2</sub>O<sub>2</sub> and were cycled between zero and 1400 mV in the background electrolyte to improve the reproducibility of the EC experiments. Voltammetric measurements were carried out in 0.01 M Na<sub>2</sub>SO<sub>4</sub> background electrolyte. The concentration of arsenite was fixed at 10<sup>−4</sup> M. The scan rate was 50 mV/s.

\* Corresponding author phone: (206)543-2394; fax: (206)685-9185; e-mail: Korshin@u.washington.edu.

<sup>†</sup> University of Washington.

<sup>‡</sup> Yeshiva University.

<sup>§</sup> Ukrainian State University of Chemical Technology.

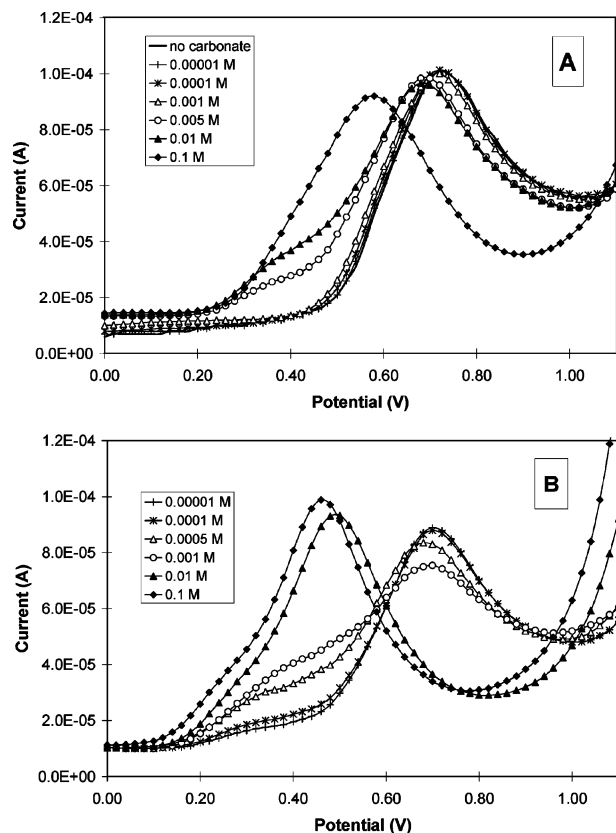


**FIGURE 1.** Effects of carbonate concentration on the EC arsenite oxidation on platinum rotating disk electrode at pH 8 (A) and 10 (B). Background electrolyte 0.01 M  $\text{Na}_2\text{SO}_4$ , arsenite concentration  $10^{-4}$  M, rotation speed 200 rpm.

XAFS measurements were performed at beamline  $\times 16\text{C}$  of the National Synchrotron Light Source at Brookhaven National Laboratory. A Si(111) double crystal monochromator was used to vary the X-ray energy from 200 eV below to 850 eV above the absorption K edge of As (11868 eV). To minimize harmonics, the monochromator crystals were detuned by about 25%. The samples were measured in fluorescence mode by using a Stern-Heald ionization detector. A germanium filter (3 absorption lengths thick) and Soller-type slits were used to minimize the scattering background. A partially transparent gas ionization chamber was used to measure the incident X-ray intensity ( $I_0$ ). To correct for a small angular drift in the position of the monochromator crystals between the scans, the data sets were carefully compared and were adjusted versus their absolute energy before the averaging. The adjustment versus absolute energy was done using the position of a sharp glitch in the  $I_0$  detector channel as a reference point and was used to vary X-ray energy. Extended X-ray absorption fine-structure (EXAFS) data were analyzed using the UWXAFS data analysis package (25). After averaging five to eight individual scans for each sample, the smooth background function was removed from the absorption coefficient data and the resultant EXAFS function was edge-step normalized. This procedure was performed by the AUTOBK program (26). Theoretical scattering amplitudes and phases of the photoelectron were calculated with the program FEFF6 (27). To analyze the data within FEFF theory, we used the program FEFFIT (25) that utilizes the nonlinear least-squares fitting of EXAFS theory to the data and evaluates uncertainties in the results. During the fits, the data and the theory were  $k^2$ -weighted and Fourier transformed using Hanning window function and  $k$ -range from 2 to  $12 \text{ \AA}^{-1}$ . The fitting ranges were from 1.0 to  $1.8 \text{ \AA}$ .

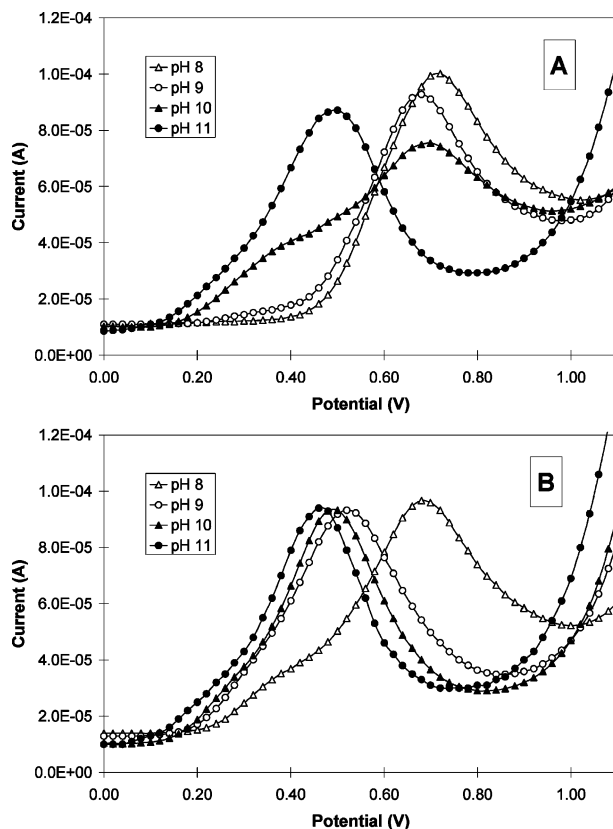


**FIGURE 2.** Effects of pH on the EC arsenite oxidation on platinum rotating disk electrode. Carbonate concentration 0.001 M (A) and 0.01 M (B). Arsenite concentration  $10^{-4}$  M, rotation speed 200 rpm.

## Results and Discussion

In the background 0.01 M  $\text{Na}_2\text{SO}_4$  electrolyte without added carbonate, EC oxidation of arsenite on platinum manifested itself as a broad peak located in the range of potentials 0.5–1.0 V (Figure 1). At  $E < 0.45$  V, the intensity of EC current associated with arsenite oxidation in the background electrolyte was virtually negligible, while the position of the arsenite oxidation peak exhibited little sensitivity to pH variations in the circumneutral range.

At increased total carbonate concentrations, the influence of pH on the EC oxidation of arsenite became more apparent. For instance, at pH 8 the increase of the total carbonate concentration from  $10^{-4}$  M to 0.1 M was accompanied by a gradual shift of the maximum of the oxidation peak ( $E_{\text{max}}$ ) from 0.72 to 0.58 V (Figure 1A). For pH 10, the shift of  $E_{\text{max}}$  values for the same range of carbonate concentrations was from 0.71 to 0.47 V (Figure 1B). The rate of arsenite oxidation for  $E < 0.45$  V also increased rapidly with the rise of carbonate concentration. For pH 8, the oxidation current at  $E > 0.20$  V was observed to increase at total carbonate concentrations  $> 10^{-3}$  M, while at pH 10 the arsenite exhibited EC activity at EC potentials  $> 0.15$  V and total carbonate concentrations as low as  $10^{-4}$  M.

Effects of total carbonate concentrations and pH on the EC arsenite oxidation on the platinum electrode are further demonstrated in Figure 2. This figure shows that for a  $10^{-3}$  M total carbonate concentration, the cathodic shift of the onset of arsenite oxidation current becomes evident at pH  $> 9$  (Figure 2A). At a 0.01 M carbonate concentration, each increment of pH  $> 8$  is accompanied by a pronounced shift of the arsenite oxidation peak (Figure 2B).

The EC oxidation of arsenite on gold exhibited trends similar to those observed for platinum, but it had additional features. The most important of them was the presence of

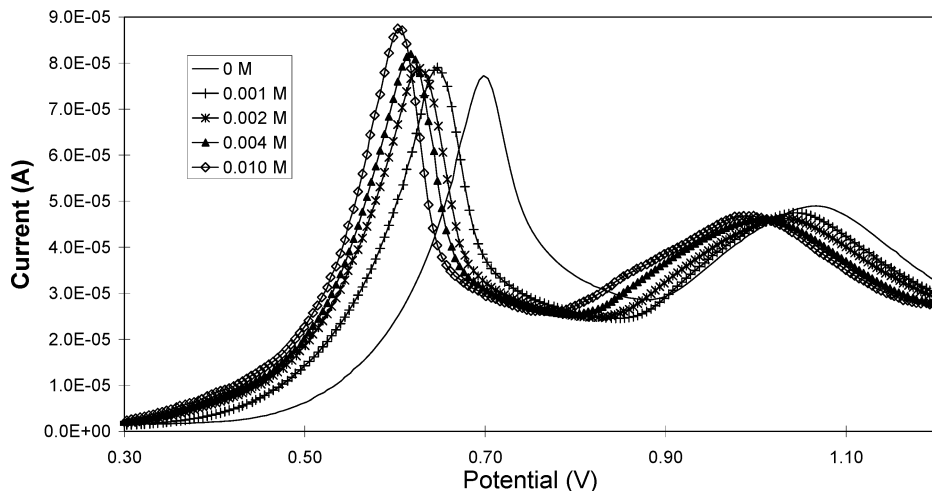


FIGURE 3. Effects of carbonate concentration on the EC arsenite oxidation on gold rotating disk electrode. pH 8, arsenite concentration  $10^{-4}$  M, rotation speed 200 rpm.

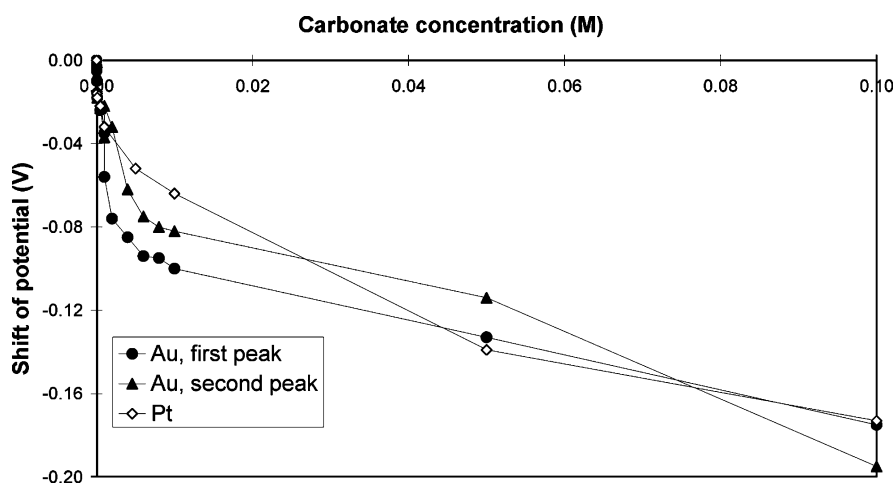


FIGURE 4. Shift of the potentials of maxima in potentiodynamic scans for gold and platinum electrodes as a function of carbonate concentration. pH 8, arsenite concentration  $10^{-4}$  M, rotation speed 200 rpm.

two well-resolved voltammetric peaks (Figure 3) similar to those observed in prior research (22–24). These peaks correspond to two one-electron-transfer steps and indicate the formation of an As(IV) intermediate. In the absence of carbonate, the first and second arsenite oxidation peaks were located in the range of potentials 0.5–0.9 V and 0.9–1.2 V, respectively.

The position of both peaks was affected by both the pH and the total carbonate concentration. Similarly to the results for platinum, the onset of arsenite oxidation exhibited a pronounced cathodic shift as the total concentration of carbonate or pH increased. For pH 8.0, the increase of added carbonate from 0 to 0.01 M was accompanied by the shift of the first voltammetric peak from 0.70 to 0.60 V, while the position of the maximum of the second peak decreased from 1.07 to 0.99 V. Despite some differences in the positions of the voltammetric peaks for the gold and platinum electrodes, effects of variations of total carbonate concentration of their shift at a constant pH were similar, as demonstrated in Figure 4 for pH 8.0.

The effects of the pH and carbonate on the EC oxidation of arsenite were quantified using the relative enhancement of arsenite oxidation current  $I/I_0$  (where  $I_0$  and  $I$  are the arsenite oxidation currents measured in the absence and presence of carbonate, respectively) at a potential for which little EC activity of arsenite is observed in the absence of carbonate. The potential of +0.50 V was selected for this purpose.

Analysis of the behavior of  $E_{\max}$  and  $I/I_0$  values for platinum in the entire range of experimental conditions showed that both  $E_{\max}$  shift and  $I/I_0$  ratios were strongly correlated only with the concentration of free carbonate ion  $\text{CO}_3^{2-}$  (Figure 5 and Figure 6). At the same time, no correlation was determined to exist between the parameters of EC arsenite oxidation and, on the other hand, pH or total concentration of carbonate or bicarbonate  $\text{HCO}_3^-$ . Data presented in Figure 6 show that the enhancement of EC oxidation of  $10^{-4}$  M arsenite becomes notable at  $\text{CO}_3^{2-}$  concentrations exceeding a certain threshold level (ca.  $10^{-4.5}$  M  $\text{CO}_3^{2-}$ ), and it tends to reach a plateau for  $\text{CO}_3^{2-}$  concentrations  $>10^{-3}$  M. This behavior can be interpreted as a manifestation of the formation of one or more arsenite–carbonate complexes that appear to be more amenable to EC oxidation than free arsenite. This hypothesis would be in agreement with the concept of arsenite–carbonate complexation presented in ref 18. Accordingly, it was hypothesized that the formation of an EC-active monocarbonate complex of arsenite (operationally denoted as  $[\text{As}(\text{III})\text{CO}_3]$ ) can explain the increase of the oxidation current at  $\text{CO}_3^{2-}$  concentrations  $>10^{-4.5}$  M. Using similar reasoning, it was suggested that an additional increase of the arsenite oxidation current at  $\text{CO}_3^{2-}$  concentrations  $>10^{-2}$  M (Figure 6) accompanied by a small but consistent cathodic shift of the  $E_{\max}$  values (Figure 5) may be interpreted as a manifestation of the formation of a dicarbonate complex of As(III) operationally denoted as  $[\text{As}(\text{III})-(\text{CO}_3)_2]$ . (The assumed stoichiometries of these complexes

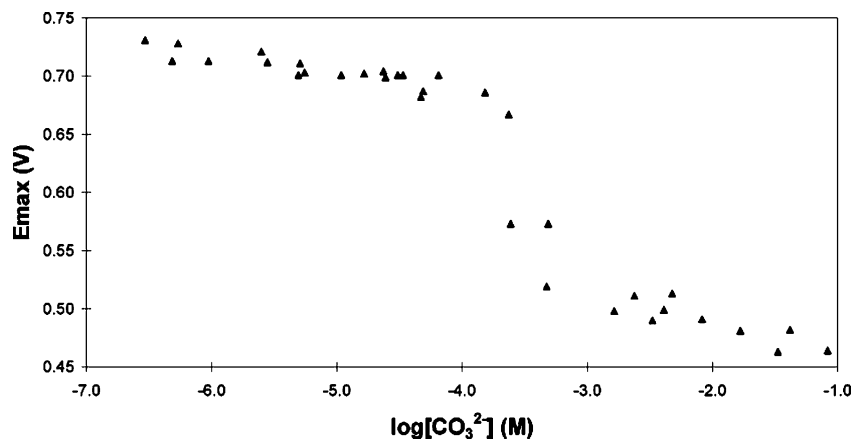


FIGURE 5. Dependence of the potential of the maximum in the potentiodynamic scans for platinum electrode as a function of free carbonate concentration. Compilation of data for pH from 8 to 11 and total carbonate concentrations from  $10^{-5}$  M to 0.1 M.

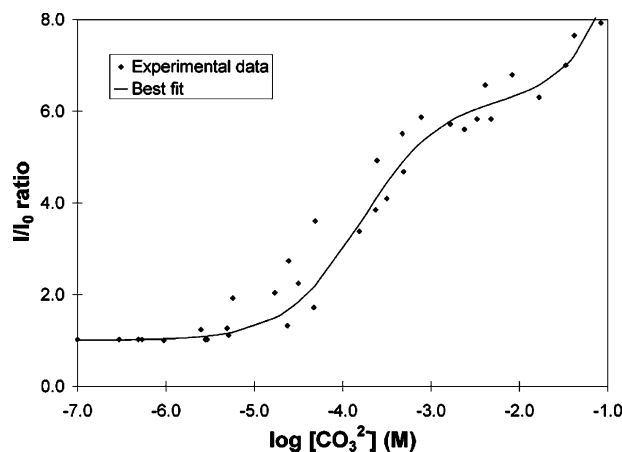


FIGURE 6. Relative enhancement of the oxidation current of arsenite as a function of free carbonate concentration. Compilation of data for platinum electrode, pH from 8 to 11, total carbonate concentrations from  $10^{-5}$  M to 0.1 M.

do not necessarily account for the actual number of OH<sup>-</sup> groups that can be present in the inner complexation shell of As(III). This issue will be addressed in the sections that follow.)

To determine the apparent formation constants for these complexes and their relative activities in EC oxidations, the data shown in Figure 6 were processed using equations that represent the enhancement of the current that corresponds to the EC oxidation of the arsenite-carbonate complexes (eq 1) and relevant mass balances in the system:

$$\frac{I}{I_0} = \frac{[\text{As(III)}]}{C_{\text{As}}} + \alpha_1 \frac{[\text{As(III)CO}_3]}{C_{\text{As}}} + \alpha_2 \frac{[\text{As(III)(CO}_3)_2]}{C_{\text{As}}} \quad (1)$$

$$C_{\text{As}} = [\text{As(III)}] + [\text{As(III)CO}_3] + [\text{As(III)(CO}_3)_2] \quad (2)$$

$$C_{\text{carb}} = [\text{H}_2\text{CO}_3] + [\text{HCO}_3^-] + [\text{CO}_3^{2-}] + [\text{As(III)CO}_3] + 2[\text{As(III)(CO}_3)_2] \quad (3)$$

$$[\text{As(III)CO}_3] = \beta_1 [\text{As(III)}][\text{CO}_3^{2-}] \quad (4)$$

$$[\text{As(III)(CO}_3)_2] = \beta_2 [\text{As(III)}][\text{CO}_3^{2-}]^2 \quad (5)$$

In these equations,  $\alpha_1$  and  $\alpha_2$  are the relative EC activities of mono- and dicarbonate complexes of As(III), and  $\beta_1$  and  $\beta_2$  are the formation constants of these complexes. As(III) in the above equations corresponds to all species of free arsenite without distinguishing their protonation status.

Fitting the  $I/I_0$  data shown in Figure 6 indicated that the formation constant for the monocarbonate complex of arsenite was  $6100 \pm 800 \text{ M}^{-1}$ , while the value of  $\alpha_1$  (the relative enhancement of the oxidation current) was  $6.2 \pm 0.6$ . The formation constant for the dicarbonate complex was only slightly higher ( $12000 \pm 1600$ ) than that of the monocarbonate complex, although the relative activity of the dicarbonate complex of As(III) in EC oxidation was almost twice as high ( $11.7 \pm 1.2$ ) as that of the monocarbonate complex.

To examine the properties of the inner complexation shell of the hypothesized As(III) complexes, EXAFS measurements for solutions containing 0.001 M arsenite and varying concentrations of carbonate were carried out. To account for the possibility of different activities of arsenite species with varying degrees of protonation, EXAFS measurements were performed at pH 8.3, 11.0, and 13.0. These pH values correspond to the predominance of  $\text{H}_3\text{AsO}_3$ ,  $\text{H}_2\text{AsO}_3^-$ , and  $\text{AsO}_3^{3-}$ , respectively. EXAFS measurements for arsenate were also obtained.

In accord with prior publications (28–30), our XAFS measurements showed that the absorption edge of As(III) in arsenite exhibited a notable shift to lower photon energies compared with EXAFS spectra of arsenate. However, the X-ray absorption near edge structure (XANES) of As(III) did not exhibit any sensitivity to the presence of carbonate even at high concentrations of the latter. This was interpreted to indicate that no carbon atoms entered the inner complexation shell of As(III) even when the postulated As(III)-complexes were likely to predominate. Indeed, if As–C bonds had been formed in any of these complexes, consistent changes in the XANES spectra of arsenic would have been observed because of the markedly different electronegativities of carbon and oxygen atoms in corresponding As model compounds (31).

Background-subtracted, edge-step normalized,  $k^2$ -weighted EXAFS data for arsenite and arsenate are shown in Figure 7, while their Fourier transform magnitudes along with the best fits obtained using FEFF6 theory are represented in Figure 8. Theoretical contributions corresponding to the first-shell signal were modeled as As–O nearest neighboring bonds. The crystal structure of scorodite ( $\text{FeAsO}_4 \cdot 2\text{H}_2\text{O}$ ) was used to generate photoelectron scattering amplitudes and phases corresponding to the As–O bonds. In the fits, the correction to the photoelectron energy origin, the model As–O distance, the standard deviation in this distance, and the coordination number of As–O first nearest neighboring bonds were varied. The total number of the fitting variables (4) was much smaller than the total number of the relevant independent data points (7). Results of the numerical processing of EXAFS data for arsenite at varying pHs and carbonate concentrations to determine effects of these parameters on the first nearest neighbors (INN) numbers, INN bond lengths and mean

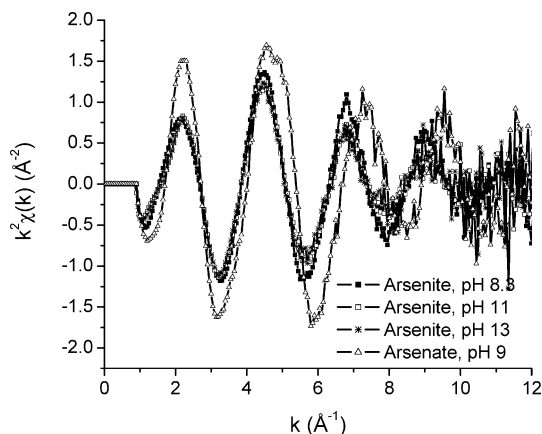


**FIGURE 7.** Background-subtracted, edge-step normalized,  $k^2$ -weighted EXAFS data for arsenite at varying pHs and zero carbonate concentration. Data for arsenate at pH 9 are also shown.

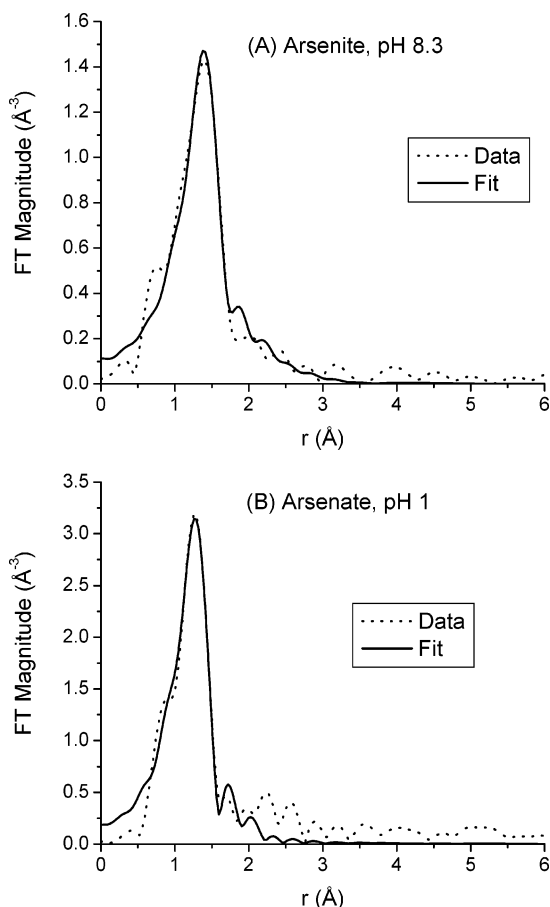


**FIGURE 8.** Fourier transform magnitudes of EXAFS data and FEFF6 fits to (A) arsenite at zero carbonate concentration at pH 8.3 and (B) arsenate at pH 1.0.

square disorders for the As–O bond in the inner shell of arsenite are shown in Table 1, Table 2, and Table 3, respectively. EXAFS results for arsenate are given in Table 4. These data are very close to those obtained in the preceding studies (28–30). They indicate that the geometry of the arsenite's inner complexation shell and strength of the As–O bonds in it are not affected by variations of carbonate concentrations or pH. In all cases, the INN number for arsenite was close to 3.0, while for arsenate the INN number was on the average 4.11. The lack of sensitivity of the parameters of the inner shell of arsenite to the presence of carbonate appears to contradict the stoichiometries and

**TABLE 1.** Effects of pH and Carbonate Concentration on the Number of Nearest Neighbors in the Inner Shell of Arsenite

carbonate concentration, M	Number of Nearest Neighbors $N_{As-O}$		
	pH		
	8.3	11.0	13.0
0.00	$3.06 \pm 0.30$	$2.93 \pm 0.34$	$3.11 \pm 0.41$
0.01	$3.08 \pm 0.30$	$3.02 \pm 0.32$	$2.84 \pm 0.26$
1.00	$3.00 \pm 0.28$	$3.04 \pm 0.38$	$2.96 \pm 0.27$

**TABLE 2.** Effects of pH and Carbonate Concentration on the Radial Arsenic–Oxygen Distances in the Inner Shell of Arsenite

carbonate concentration, M	Radial Arsenic–Oxygen Distances $R_{As-O}$ , Å		
	pH		
	8.3	11.0	13.0
0.00	$1.789 \pm 0.007$	$1.80 \pm 0.01$	$1.79 \pm 0.01$
0.01	$1.786 \pm 0.009$	$1.78 \pm 0.01$	$1.796 \pm 0.008$
1.00	$1.789 \pm 0.008$	$1.80 \pm 0.01$	$1.789 \pm 0.007$

**TABLE 3.** Effects of pH and Carbonate Concentration on Mean Square Disorder for the As–O Bond in the Inner Shell of Arsenite

carbonate concentration, M	Mean Square Disorder for Bond As–O $\sigma^2_{As-O}$ , Å <sup>2</sup>		
	pH		
	8.3	11.0	13.0
0.00	$0.0020 \pm 0.0012$	$0.0054 \pm 0.0016$	$0.0064 \pm 0.0020$
0.01	$0.0025 \pm 0.0011$	$0.0056 \pm 0.0016$	$0.0045 \pm 0.0011$
1.00	$0.0024 \pm 0.0011$	$0.0062 \pm 0.0018$	$0.0055 \pm 0.0014$

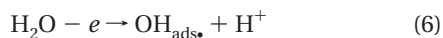
**TABLE 4.** Effects of pH on the Parameters of the Inner Shell of Arsenate

pH	$N_{As-O}$	$R_{As-O}$ (Å)	$\sigma^2_{As-O}$ (Å <sup>2</sup> )
1.0	$4.19 \pm 0.28$	$1.699 \pm 0.005$	$0.0025 \pm 0.0007$
5.0	$4.29 \pm 0.22$	$1.695 \pm 0.004$	$0.0034 \pm 0.0006$
9.0	$3.86 \pm 0.16$	$1.702 \pm 0.003$	$0.0019 \pm 0.0004$

values of formation constants hypothesized in ref 18. For instance, assuming that the EC data discussed above indicate the prevalence of a monocarbonate complex at sufficiently high concentrations of  $CO_3^{2-}$ , the constant INN value for the inner complexation shell of As(III) indicates that the actual composition of that complex is almost certainly either  $[As(OH)(CO_3)]^0$  or  $[As(OH)_2(CO_3)]^-$  rather than  $[AsCO_3]^+$ .

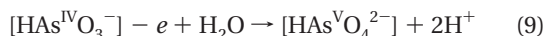
The nearly constant  $\sigma^2_{As-O}$  values at varying pHs and carbonate concentrations indicate that the strength of bond between an arsenic (oxidation state +3) and the oxygen atom in a hydroxyl group of the inner complexation shell is essentially the same as that between  $As^{3+}$  and the oxygen atom in a carbonate group. This would indicate a weak preference of binding of carbonate versus that of  $OH^-$ . The absence of evidence of a fourth oxygen atom in the inner complexation shell of As(III) even at very high concentrations of carbonate (Table 1) indicates that if a dicarbonate complex of As(III) ( $[As(CO_3)_2]^-$ ) is formed, only one bound bicarbonate can interact with the central As atom via bidentate configuration, while the second carbonate group can be bound only via monodentate ligation. The assumption of a weak ligation of the second carbonate group in the bicarbonate complex of As(III) also concurs with a very small increment of the formation constant for the dicarbonate complex compared to that of the monocarbonate complex of As(III) ( $\beta_2$  and  $\beta_1$  values are 12 000 and 6100, respectively).

Alternatively, the constancy of the parameters of the inner complexation shell of arsenite at high levels of carbonate can be interpreted as a manifestation of a complete absence of specific carbonate–arsenite interactions. In that case, a question arises: what is the mechanism of the carbonate acceleration of EC arsenite oxidation? One mechanism that might be considered to explain the observed phenomena is that the oxidation of arsenite proceeds via the EC formation of OH• or CO<sub>3</sub><sup>•-</sup> radicals and that CO<sub>3</sub><sup>•-</sup> might play a specific role in the acceleration of the oxidation of arsenite. Indeed, OH• radicals can be generated via the following EC reactions observed for many types of electrodes (23, 24, 32, 33):

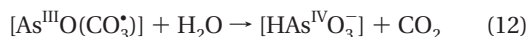
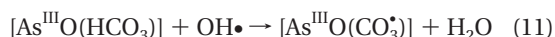


EC-generated OH• radicals can also interact with the species of carbonate to produce carbonate-radical CO<sub>3</sub><sup>•-</sup>. To account for the observed acceleration of the EC oxidation of arsenite at increased carbonate and pH levels, it would be necessary to assume that the rate of reaction between CO<sub>3</sub><sup>•-</sup> and arsenite species is higher than that for OH•. However, this assumption is unlikely to be correct. First, CO<sub>3</sub><sup>•-</sup> is less reactive than hydroxyl radical, and this was confirmed for the oxidation of arsenite in the radiolysis studies (21). Second, if the formation of CO<sub>3</sub><sup>•-</sup> precedes the EC oxidation of the arsenite, then it is not clear why it is only the concentration carbonate ion CO<sub>3</sub><sup>2-</sup> that is unambiguously correlated with the values of E<sub>max</sub> and I/I<sub>0</sub>. Indeed, CO<sub>3</sub><sup>•-</sup> can be formed via interactions of OH• with all species of carbonic acid. This would have resulted in a correlation between total carbonate concentrations (rather than those of CO<sub>3</sub><sup>2-</sup> only) and acceleration of EC arsenite oxidation, but no such fact was observed.

In all, the results outlined above appear to indicate that arsenite forms relatively weak mono- and bicarbonate complexes that are more amenable to EC oxidation. It can be hypothesized that the reason for the observed acceleration is that in reactions with OH• species, carbonate–arsenite complexes have more electron donors than free arsenite. For arsenite per se, EC reactions can be written, in agreement with (21–24), as a sequence of two electron transfers:



In the presence of the carbonate complexes (e.g., [As(OH)(CO<sub>3</sub>)]<sup>0</sup> or [As(OH)<sub>2</sub>(CO<sub>3</sub>)]<sup>-</sup>), additional oxidation pathways can exist. For instance, because the carbonate group can also provide an electron to reduce OH• and thereby form a transient radical group that is a part of the inner complexation shell of As(III), the formation of As(IV) can also proceed via the following sequence of reactions:



In the above reactions, the carbonate serves as a bridge to transfer an electron from As(III) to OH•, and it also provides a molecule of CO<sub>2</sub>, an excellent leaving group, in the reaction step that yields As(IV). Similar reaction sequences in which the carbonate group provides an intermediate source of

electrons and an easily released leaving group can take place for other As(III) complexes ([As(OH)<sub>2</sub>(CO<sub>3</sub>)]<sup>-</sup> and [As(CO<sub>3</sub>)<sub>2</sub>]<sup>-</sup>).

The EC data also indicate that the oxidation of As(IV) does not seem to be specifically promoted by carbonate. Indeed, the shift of the E<sub>max</sub> values for the second peak in the potentiodynamic scans on the gold electrolyte is practically the same as that of the first peak (Figure 4), while the overall shape of the peak associated with the oxidation of As(IV) to As(V) does not show any notable changes associated with the presence of carbonate (Figure 3). Therefore, the oxidation of As(IV) to As(V) is likely to proceed either via a one-electron transfer (eq 9) or via EC-generated OH• radicals:



As discussed in ref 21, As(IV) can also disappear via disproportionation to form As(III) and As(V):



## Acknowledgments

This study was partially supported by Awwa Research Foundation (project # 2728). A.I.F. acknowledges support by the U.S. Department of Energy Grant No. DE-FG02-03ER15477; NSLS is supported by the Divisions of Materials and Chemical Sciences of DOE. The views represented in this publication do not necessarily represent those of the funding agency. The authors also would like to thank Prof. James M. Mayer, Chemistry Department of University of Washington, for his valuable contribution in the discussions concerning the chemistry of carbonate–arsenite interaction.

## Literature Cited

- Smedley, P. L.; Kinniburgh, D. G. A review of the source, behavior and distribution of arsenic in natural waters. *Appl. Geochem.* **2002**, *17* (5), 517–568.
- Berg M.; Tran, H. C.; Nguyen, T. C.; Pham H. V.; Schertenleib, R.; Giger, W. Arsenic contamination of groundwater and drinking water in Vietnam: a human health threat. *Environ. Sci. Technol.* **2001**, *35* (13), 2621–2626.
- Vagliasindi, F. G. A.; Benjamin, M. M. Arsenic removal in fresh and NOM-preloaded ion exchange packed bed adsorption reactors. *Water Res. Technol.* **1998**, *38* (6), 337–343.
- Chen, H. W.; Frey, M. M.; Clifford, D.; McNeill, L. S.; Edwards, M. A. Arsenic treatment considerations. *J. AWWA* **1999**, *91* (3), 74–85.
- Bissen, M.; Frimmel, F. H. Arsenic – A Review. Part II. Oxidation of arsenic and its removal in water treatment. *Acta Hydrochim. Hydrobiol.* **2003**, *31* (2), 97–107.
- Farrell, J.; Wang, J.; O'Day, P.; Conklin, M. Electrochemical and spectroscopic study of arsenate removal from water using zero-valence iron media. *Environ. Sci. Technol.* **2001**, *35* (10), 2026–2032.
- Driehaus, W.; Seith, R.; Jekel, M. Oxidation of arsenate (III) with manganese oxides in water treatment. *Water Res.* **1995**, *29* (1), 297–305.
- Kim, M. J.; Nriagu, J. Oxidation of arsenite in groundwater using ozone and oxygen. *Sci. Total Environ.* **2000**, *247* (1), 71–79.
- Hug, S. J.; Canonica, L.; Wegelin, M.; Gechter, D.; von Gunten, U. Solar oxidation and removal of arsenic at circumneutral pH in iron containing waters. *Environ. Sci. Technol.* **2001**, *35* (10), 2114–2121.
- Voegelin, A.; Hug, S. J. Catalyzed oxidation of arsenic (III) by hydrogen peroxide on the surface of ferrihydrite: an in situ ATR-FTIR study. *Environ. Sci. Technol.* **2003**, *37* (5), 972–978.
- Hug, S. J.; Leupin, O. Iron-catalyzed oxidation of arsenic (III) by oxygen and by hydrogen peroxide: pH-dependent formation of oxidants in the Fenton reaction. *Environ. Sci. Technol.* **2003**, *37* (12), 2734–2742.
- Emett, M. T.; Khoe, G. H. Photochemical oxidation of arsenic by oxygen and iron in acidic solutions. *Water Res.* **2001**, *35* (3), 649–656.
- Arienzo, M.; Adamo, P.; Chiarenzelli, J.; Bianco, M. R.; De Martino, A. Retention of arsenic on hydrous ferric oxides generated by electrochemical peroxidation. *Chemosphere* **2002**, *48* (10), 1009–1018.

- (14) Korshin, G. V.; Kim, J.; Velichenko, A. B. *Development of an Electrochemical System for Arsenite Oxidation in Drinking Water*; Awwa Research Foundation: Denver, CO, 2004.
- (15) Nickson, R. T.; McArthur, J. M.; Ravenscroft, P.; Burgess, W. G.; Ahmed, K. M. Mechanisms of arsenic release to groundwater, Bangladesh and West Bengal. *Appl. Geochem.* **2000**, *15* (4), 403–413.
- (16) Anawar, H. M.; Akai, J.; Sakugawa, H. Mobilization of arsenic from subsurface sediments by effects of bicarbonate ions in groundwater. *Chemosphere* **2004**, *54* (6), 753–762.
- (17) Appelo, C. A. J.; Van der Weiden, M. J. J.; Tournassat, C.; Charlet, L. Surface complexation of ferrous iron and carbonate on ferrihydrite and the mobilization of arsenic. *Environ. Sci. Technol.* **2002**, *36* (14), 3096–3103.
- (18) Kim, M. J.; Nriagu, J.; Haack, S. Carbonate ions and arsenic dissolution by groundwater. *Environ. Sci. Technol.* **2000**, *34* (15), 3094–3100.
- (19) Woods, R.; Kolthoff, I. M.; Meehan, E. J. Arsenic (IV) as an intermediate in the induced oxidation of arsenic (III) by iron (II)-persulfate reaction and the photoreduction of iron (III). 1. Absence of oxygen. *J. Am. Chem. Soc.* **1963**, *85* (16), 2385–2390.
- (20) Daniels, M. Photochemically induced oxidation of arsenite: evidence for the existence of As (IV). *J. Phys. Chem.* **1962**, *66* (8), 1473–1475.
- (21) Klaning, U.K.; Bielski, B. H. J.; Sehested, K. Arsenic (IV) – a pulse radiolysis study. *Inorg. Chem.* **1989**, *28* (14), 2717–2724.
- (22) Catherino, H. A. The electrochemical oxidation of arsenic (III): a consecutive electron-transfer reaction. *J. Phys. Chem.* **1967**, *71* (2), 268–274.
- (23) Zakharov, V. A.; Songina, O. A.; Kalnitskaya, L. P. Studies of electrochemical behavior of arsenite on a gold electrode. *Sov. J. Electrochem.* **1971**, *17*, 1702–1704.
- (24) Mustafa, I. A.; Igumnov, M. S.; Rysev, A. P. Some specific features of the electrochemical behavior of arsenite ions at a rotating platinum electrode studied by cyclic voltammetry. *J. Anal. Chem.* **1997**, *52* (10), 987–991.
- (25) Stern, E. A.; Newville, M.; Ravel, B.; Yacoby, Y.; Haskel, D. The UWXAFS analysis package: philosophy and details *Physica B (Amsterdam)* **1995**, *208/209*: 117–120.
- (26) Newville, M.; Livins, P.; Yacoby, Y.; Rehr, J. J.; Stern, E. a. Near-edge X-ray absorption fine structure of Pb: A comparison of theory and experiment. *Phys. Rev. B* **1993**, *47*, 14126–14131.
- (27) Zabinsky, S. I.; Rehr, J. J.; Ankudinov, A.; Albers, R. C.; Eller, M. J. Multiple-scattering calculations of X-ray-absorption spectra. *Phys. Rev. B* **1995**, *52* (4), 2995–3009.
- (28) Foster, A. L.; Brown, G. E.; Tingle, T. N.; Parks, G. A. Quantitative arsenic speciation in mine tailings using X-ray absorption spectroscopy. *Am. Mineral.* **1998**, *83* (5/6), 553–568.
- (29) Arai, Y.; Elzinga, E. J.; Sparks, D. L. X-ray absorption spectroscopic investigation of arsenite and arsenate adsorption at the aluminum oxide-water interface. *J. Colloid Interface Sci.* **2001**, *235* (1), 80–88.
- (30) Farquhar, M. L.; Charnock, J. M.; Livens, F. R.; Vaughan, D. J. Mechanisms of arsenic uptake from aqueous solutions by interaction with goethite, lepidocrocite, mackinawite and pyrite: an X-ray absorption spectroscopy study. *Environ. Sci. Technol.* **2002**, *36* (8), 1757–1762.
- (31) Norman, N. C. *Chemistry of Arsenic, Antimony, and Bismuth*; Blakie Academic and Professional: New York, 1998.
- (32) Janssen, L. J. J.; Vanderheyden, P. D. L. Mechanism of anodic oxidation of chlorate to perchlorate on platinum electrodes. *J. Appl. Electrochem.* **1995**, *25* (2), 126–136.
- (33) Martinez-Huitle, C. A.; Ferro, S.; De Battisti, A. Electrochemical incineration of oxalic acid – Role of electrode material. *Electrochim. Acta* **2004**, *49* (22/23), 4027–4034.

Received for review August 24, 2005. Revised manuscript received October 25, 2005. Accepted November 2, 2005.

ES0516817